Experimental Assessment of Induced Voltage in a Scaled Building Directly Hit by Lightning

Camila A. Dias, Ronaldo K. Moreira, Rose M. Batalha
Programa de Pós Graduação em Engenharia Elétrica
PUC Minas
Belo Horizonte, Brasil
camilaaparecidadias@gmail.com, rkascher@kascher.com.br

Hudson R. Soares, Eduardo E. Cardoso
Instituto Politécnico
PUC Minas
Belo Horizonte, Brasil
hudsonrodrigo153@gmail.com, eugenio-fox@hotmail.com

***Abstract*— The strike of lightning directly or even nearby an electrical installation produces electromagnetic pulses and consequently induces over voltages on equipment ports inside a building structure. From an electromagnetic compatibility point of view, knowledge of the magnetic fields in the internal structures is essential for the development of protective systems against surges. This paper presents an experimental evaluation of the shielding efficiency provided by different LPS configurations, to the magnetic field developed inside a structure hit by a direct lightning. Three different LPS settings were tested by changing the mesh sizes of the protection system. Measurements of the magnetic fields were carried out with a loop antenna. The building was made in a 1:20 scale wood structure. For the simulation of the lightning, a surge generator was used located at the top of the building. The measured values were compared with the ones calculated according to IEC 62305-4 and are in very good agreement.**

Keywords— Lightning Protection System, LPS, Induced voltage, IEC-62305-4, Magnetic field shielding, Electromagnetic Compatibility.

I. INTRODUCTION

Society is more and more dependent on services provided by electric and electronic systems. These systems are vital for data processing and storage, as for industrial control systems and security process. They are also crucial for establishing telecommunication services and for controlling the energy supply's infrastructure [1]. Flaws in these systems, caused by magnetic field effects from lightning strikes, may lead to severe consequences and inestimable losses. This issue was acknowledged by international institutes, which in turn established some standards, like the IEC 62305-4 [2] which addresses safety/protectives procedures in order to reduce the risk of damages caused by Lightning Electromagnetic Pulses (LEMP). Similarly, ITU-T K.20 [3] and ITU-T K.21 [4] deal with recommendations for performing surge tests on telecommunication electronic equipment. In Brazil, on June 22nd of 2015, came into effect, the new Brazilian standard NBR-5419 [5] concerning protection against lightning, whose Part 4 details procedures designed for protecting electric and electronic systems inside structures.

A magnetic field is generated in the internal structure of a building when an lightning hits, directly or indirectly, the LPS of the structure [6]-[10]. Direct lightning current generate greater magnetic fields, due to the distribution of the strike's current through the conductors that make up the LPS. On the other hand, indirect lightning strikes occur more frequently, given a higher probability of hitting a larger area around the structure, as opposed to hitting the structure itself. The internal electric and electronic systems are usually connected through wirings, which lead to the formation of induction loops. These loops can be identified in the conductors responsible for powering, grounding and for data transmission [11]. These same loops, under time variant magnetic fields, induce voltages responsible for causing interference or damages to the equipment [12]-[15].

IEC 62305-4 recommends creating Lightning Protection Zones (LPZ) against lightning strikes. These zones not only mean to mitigate the transitory effects transferred to the installation's wirings, but also to shield the same structure from the effects of the magnetic fields caused by the lightning current on the LPS. The metallic structural components of the concrete walls can be used as the limit between LPZ0 and LPZ1, and its configuration can reduce the inducing magnetic field [16]-[18]. More sensitive equipment require additional LPZs.

To determine the efficiency of the magnetic shielding provided by a LPS, a four-story building model was created on a scale factor of 1:20. The building was then equipped with a Lightning Protection System (LPS) of a variety of arrangements. The LPS was activated by an impulsive current generator, whose characteristics are similar to that of a lightning strike, within the proportionate scale. The experiments were conducted in order to evaluate three aspects:

- The lightning current distribution along the LPS conductors.
- The change in induced voltage strength in different positions of the building.
- The internal magnetic field attenuation with the use of a denser mesh provided by the horizontal and vertical LPS conductors.

Results were compared to the ones predicted in the IEC 62305-4 standard.

II. Guidelines for Testing According to IEC 62305- 4

The international standard IEC 62305-4 outlines the procedures for experimental evaluation of the magnetic field developed in the internal volume of the structure due to a direct lightning strike. Following the procedures, initially an impulse current generator with low amplitude and the shape of a typical lightning current is connected to a LPS arrangement as shown in Fig. 1.

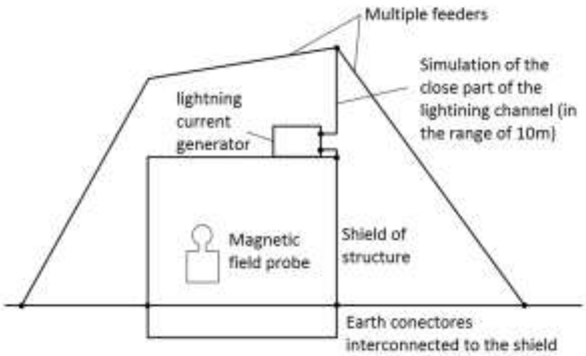

Fig. 1. LPS test arrangement with the injection of impulse current IEC 62305-4.

The impulsive voltages coupled to the internal equipment are evaluated by the time derivative of the magnetic flux caused by the lightning currents in the LPS conductors that pass through the loop area formed by the electrical wirings connected to the equipment. According to IEC 62305-4, for evaluation purpose, the loop may be considered a rectangular area with equivalent dimensions of a real loop, according to Fig. 2

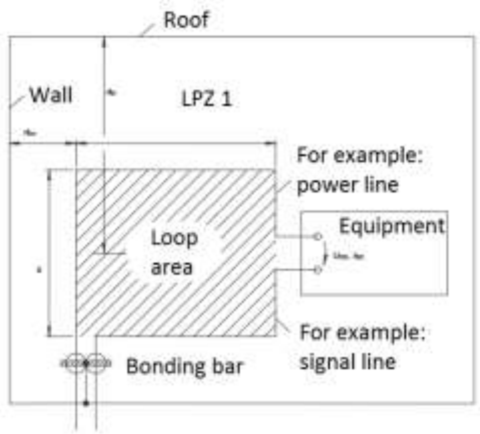

Fig. 2. Loop arrangement for the purposes of evaluating induced voltage IEC 62305-4.

III. Tests Performed

A. Reduced Scaled Structure

A 1:20 scale wooden model was used to represent a building dotted with LPS (Fig. 3). The tested arrangement had the dimensions of 50cm width, 50cm length, 60cm height, corresponding to a 10m width, 10m length, 12m height real building. The LPS was excited with a surge generator, with an impulsive peak current of 8.2A and rise time of 250ns, representing a real rise time of 5μs, according to the scale factor.

Three types of LPS arrangements have been defined for the structure showed in Fig. 4, by changing the number of down and horizontal conductors, as described in TABLE I.

Fig. 3. Models in reduced scale (a) front side (b) back side

TABLE I. Characteristics of three arrangemets

Arrangement	Number of down conductors	Number of horizontal conductors (rings)	Mesh dimensions building
1º	4	1	0.60m x 0.50m
2º	8	2	0.30m x 0.25m
3º	16	4	0.15m x 0.125m

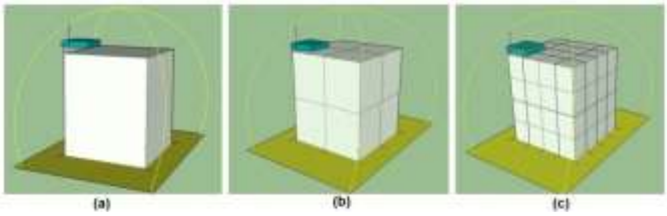

Fig. 4 Detail of the 3 LPS arrangements tested (a) 1st arrangement (b) 2nd arrangement (c) 3rd arrangement.

B. The surge current generator

The schematic representation of the surge current generator used in the tests is shown in Fig. 5.

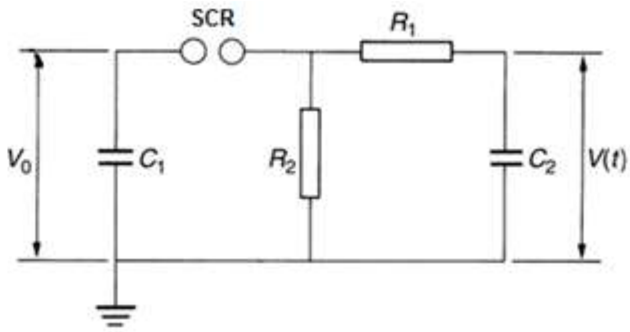

Fig. 5 Current surge generator diagram used.

By adjusting the values of R1 and C2, the front wave time is adjusted. The components C1 and R2 set the wave tail decay time. The generator is powered by a 12VDC battery, supplying a 250ns front time, 8.2A impulsive current wave.

C. *Description of the measurements*

The measurements were performed using the rectangular loop sensor illustrated in Fig. 6(a) with dimensions of 9.5 cm by 6.5 cm.

The voltages developed in the sensor were measured with an oscilloscope Agilent - model 54615B, with 500MHz bandwidth and input impedance of 50 ohms. The impulsive current injected to the structure was measured using a Pearson sensor - model 6595 with factor 0.5 V/A, see Fig. 6(b), connected to the oscilloscope second channel. This channel controlled the oscilloscope trigger, which resulted in synchronized loop voltage and current injected oscillograms.

Fig. 6. (a)Loop sensor and (b)Current sensor.

The positions of the loop voltage sensor are showed in Fig. 7 for the first and third floors of the structure.

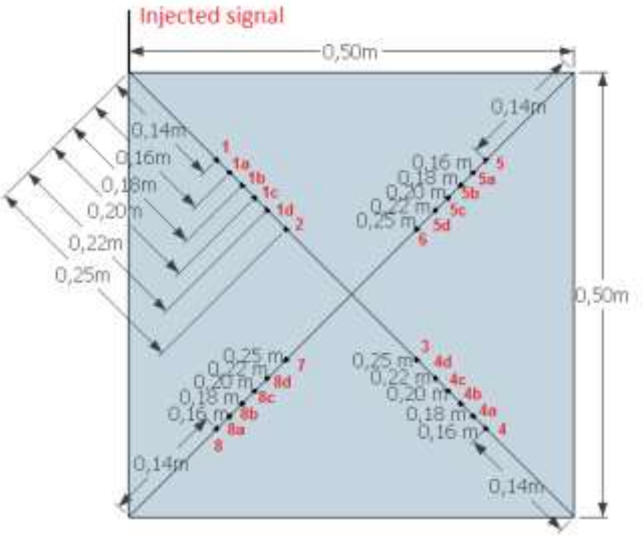

Fig. 7. Map of the sensor positions on the first and third floors.

IV. Results

A. *Assessment of current distribution in the arrangement*

The current distribution through the LPS conductors is important for the reduction of the magnetic fields generated by the lightning current, and therefore, for the reduction of the impulsive voltage applied to equipment inside the structure.

The peak current injected in the structure by the pulse generator and the current distribution was measured in arrangement 2, composed by 8 down conductors. Fig. 8 shows the current measurements points. The total injected current was 8,2A, 250ns front time.

Fig. 9 shows the injected current oscilogram. The measured value was approximately 4.1 Volts, showing, according to the measurement factor, a peak current of 8.2A.

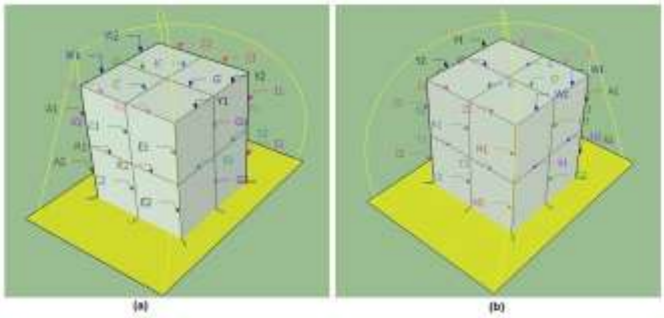

Fig. 8. Map of sensor positions on floors 1 and 3.

Fig. 9. Injected signal.

The total injected current was 8.2A and current measured in the vertical conductor below the injection point was 2.8A (conductor "A1"), which is 34.4% lower, i.e.

$$\frac{2.8}{8.14}\cdot 100=34.4\% \quad (1)$$

The current in the conductor "A2" was 1.76A, or 21.62% lower than the total current injected, i.e.

$$\frac{1.76}{8.14}\cdot 100=21.62\% \quad (2)$$

According to IEC 62305-3, the current distribution coefficient for the last floor is given by 3:

$$K_{c1}\ (n)=\frac{1}{2\cdot n}+0.1+0.2\cdot\sqrt[3]{\frac{c}{h}} \quad (3)$$

And for the one before the last floor is given by 4:

$$K_{c2}\ (n)=\frac{1}{n}+0.1 \quad (4)$$

where:

n = number of down conductors; c = distance between down wires; h = height of down conductors. This parameters for the arrangement 2 are: n = 8; c = 0.25 (m); h = 0.3 (m). And therefore, K_{c1} = 0.35 (35%) and K_{c2} = 0.225 (22,5%).

The measured and calculated coefficients are presented in Fig. 10. It can be observed, the measurements converged to the calculations considering the deviations shown in TABLE II.

TABLE II. CURRENT DISTRIBUTION IN PERCENTAGE LPS.

Calculated	Measured	Deviation
35.00%	34.40%	1.71%
22.50%	21.6%	4%

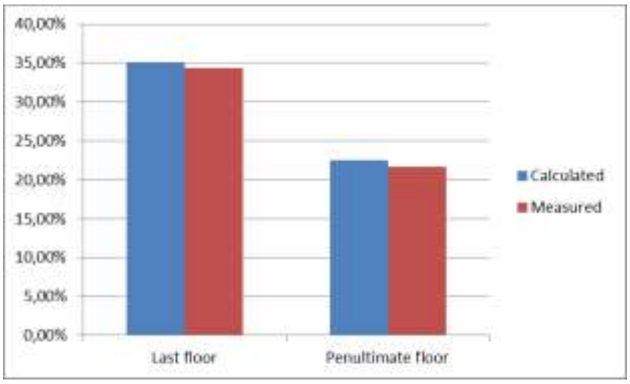

Fig. 10. Distribution of calculated and measured currents.

B. Variation of voltage induced in the loop by changing its position inside the structure

In case of a direct stroke in LPS, the magnetic field developed inside the structure will decrease with the distance from the down and captor conductors.

The analysis of the reduction of the magnetic field inside the structure was done by measuring the induced voltage as the loop is moved away from the LPS. The Fig. 11 present the loop voltage oscillogram in one point of measurement. The

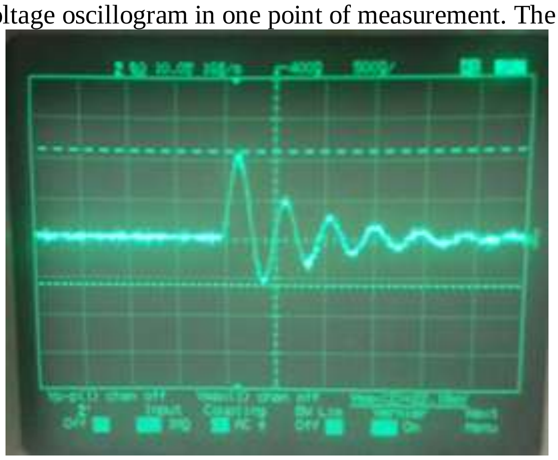

Fig. 11. Induced voltage in the loop.

following graphs represent the relative voltage attenuation factor as the internal measurement points move away from the down conductors. This factor was obtained by dividing the difference between the voltages measured at the point and at the reference point by the voltage measured at the reference point.

Figures 12 and 13 represent for the three LPS arrangements the attenuation factor for the first and third floor, respectively. The points were located according to Fig. 7.

The following figures show the average attenuation factor considering the three arrangements on the first floor (Fig.14) and on the third floor (Fig.15) referred to points 5 and 8.

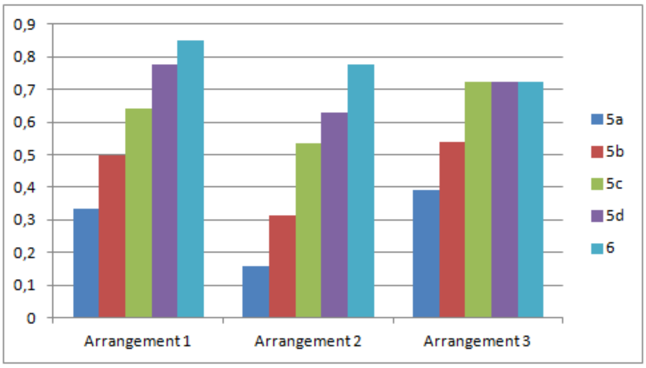

Fig. 12. Attenuation factor on the first floor referred to point 5.

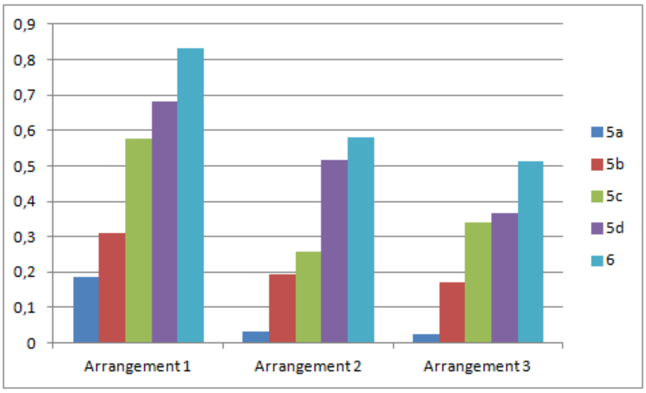

Fig. 13. Attenuation factor on the third floor referred to point 5.

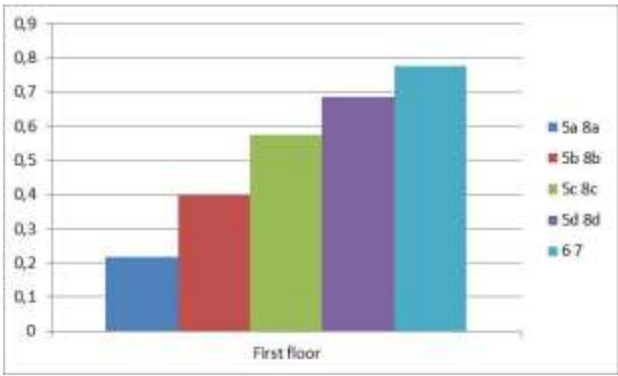

Fig. 14. Average attenuation factor in refereed to points 5 and 8 on the first floor.

We observe the increase of the attenuation factor by moving the loop away from the LPS, as it is predicted in the IEC 62305-4. This standard estimates the voltage induced in the loop by a direct lightning strike according to 5:

$$U_{ocMax}=\mu_0 \cdot b \cdot \ln\left(1+\frac{l}{d_{\frac{l}{w}}}\right)\cdot k_h \cdot \left(\frac{w}{\sqrt{d_{lr}}}\right)\cdot \frac{i_{o/max}}{T_1} \qquad (5)$$

Where:

U_{ocMax} (V) is maximum induced voltage; μ_0 (H/m) is the magnetic permeability of air equal to $4\pi 10^{-7}$; b(m) is the width of the loop; l(m) is the length of the loop; $d_{l/w}$ (m) is the distance from the building wall to the loop; k_h $(1/\sqrt{m})$ is the configuration factor, $k_h = 0.01$; w (m) is the width of the mesh in the shield-shaped grid; $d_{1/r}$ (m) is the average distance from the building roof to loop; $i_{o/Max}$ (A) is the maximum current of lightning; T_1 (s) is the lightning wavefront time.

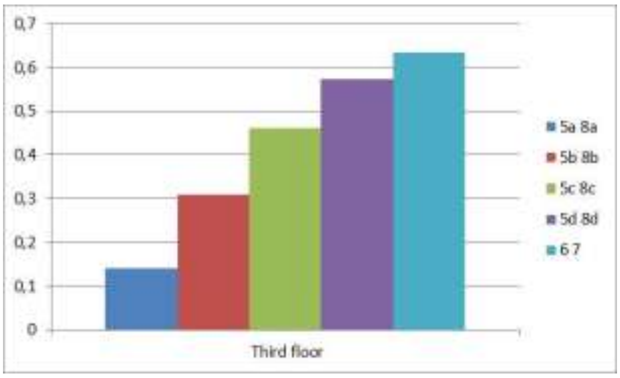

Fig. 15. Average attenuation in refereed to points 5 and 8 on the third floor.

Fig. 16 shows the attenuation of the normalized induced voltages for measured and calculated values in point 4 in the second arrangement. The measured and calculated values deviations are shown in Table III.

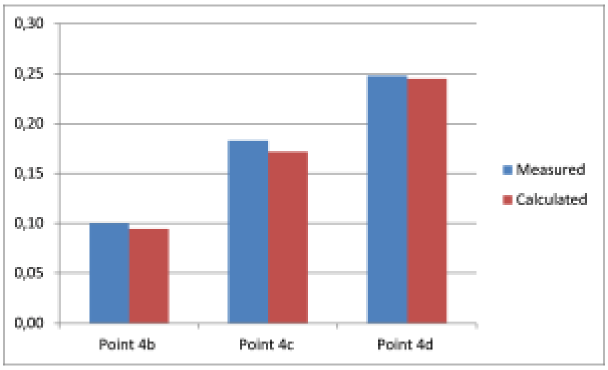

Fig. 16. Measured and calculated factor attenuation referred to point 4a.

TABLE III. DEVIATIONS BETWEEN MEASURED AND CALCULATED VALUES.

Calculated	Measured	Deviation
10.00%	9.4%	6%
18.30%	17.17%	6.17%
24.80%	24.50%	1.20%

It was then demonstrated that when the loop is moved away from the LPS conductors, the attenuation of the induced voltages is more pronounced, following the tendency estimated in IEC 62305-4.

C. Induced Voltage Reduction by reducing the LPS mesh size

According to IEC 62305-4, more significant attenuation for the internal magnetic fields is obtained with smaller mesh size provided by a greater number of the LPS captors and down conductors. To prove that it was calculated the induced voltage attenuation factor from the measurements obtained in arrangements 2 (mesh dimensions: 30 cm x 25) and 3 (mesh dimensions: 15cm x 12.5cm), based on the induced voltage obtained in arrangement 1 (mesh dimensions: 60cm x 50cm). The attenuation factors are presented in Fig. 17 (first floor) and Fig. 18 (third floor).

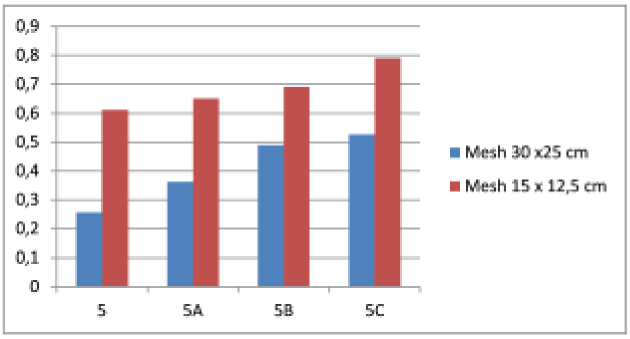

Fig. 17. Attenuation factor of the 2nd and 3rd arrangement in relation to the 1st arrangement on the first floor.

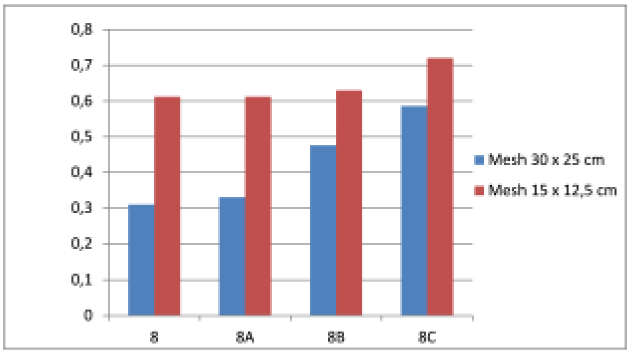

Fig. 18. Attenuation factor of the 2nd and 3rd arrangement in relation to the 1st arrangement on the third floor.

The IEC 62305-4 estimates the internal magnetic field inside LPZ1 according to 6.

$$H_1=k_h \cdot I_0 \cdot \frac{w}{d_w \cdot \sqrt{d_r}} \qquad (6)$$

where:

k_h $(1/\sqrt{m})$ is the configuration factor, k_h = 0.01. I_0 (A) is the current of the lightning discharge in the LPZ 0A; w (m) is the mesh width hof LPS; d_w (m) is the distance from the loop to the shield wall; d_r (m) is the average distance from the loop to the roof.

The above expression is valid for loops distant from the LPS corresponding to at least one mesh size formed by captors and down conductors. The field is proportional to the mesh size "w" of the LPS. Considering that the voltage induced in the loop is proportional to the magnetic field intensity, the attenuation factors of 0.5 and 0.75, respectively, for the arrangements 2 and 3, were obtained, as calculated below in 7. See mesh size in TABLE I.

$$\frac{0.5-0.25}{0.5} = 0.5 \qquad \frac{0.5-0.125}{0.5} = 0.75 \qquad (7)$$

Fig. 19 presents the average attenuation factors for the measured and calculated internal magnetic field, for arrangements 2 and 3, referred to arrangement 1, at points 5 and 8.

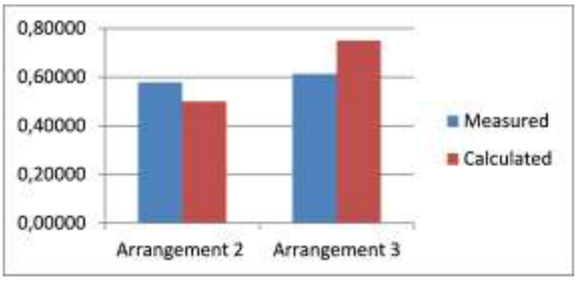

Fig. 19. Average measured and calculated reduction factors of the arrangements 2 and 3 in relation to the arrangement 1.

A good attenuation factor of the fields in arrangement 3 compared with that obtained in arrangement 2 is observed, proving the beneficial effect of using LPS with smaller mesh dimension.

The measurements obtained in arrangement 3 showed appreciable deviations compared to the calculated values. The measured voltages in this arrangement had very low amplitudes, due to the shielding influence, affecting the measurement accuracy.

The measured and calculated values deviations are shown in TABLE IV.

TABLE IV. MEASURED AND CALCULATED REDUCTION FACTORS OF THE MAGNETIC FIELD FOR THE 2 AND 3 ARRANGEMENTS

Calculated	Measured	Deviation
50.00%	57.79%	13.48%
75.00%	61.33%	18.23%

V. CONCLUSION

The international standard IEC 62305 in Part 4 deals specifically with the electric and electronic protection systems of internal structures. This standard presents the formulae for calculating the internal magnetic fields induced inside the protected building, as well as the voltages and currents coupled to the internal equipment. This work, using a scaled model, asserts the calculations proposed by IEC 62305-4. Through experimental results, the following benefits are confirmed: the distribution of the lightning's current through the LPS conductors; the reduction of the internal magnetic field when the loop is moved away from the building's roof and outer surface; as well as the magnetic field reductions when the LPS's mesh size decreases.

Presently, the authors are working on computational simulations of the scaled model used in the experiments. The goal is to investigate other factors that might influence the induced voltages caused by lightning strikes inside a structure. The analysis will take in consideration the type of lightning stroke (positive, negative and subsequent negative); the location of the stroke incidence on the LPS (corner, center, lateral); the LPS horizontal conductors; the propagation velocity of the return stroke; double layer shielding; among others.

REFERENCES

[1] E. Gohara, N. Inami, T. Tanaka, A. Sato, N. Morii, Y. Nakatsuka, and K. Hirose, “A practical approach of lightning protection measures for power receiving facilities in telecom building,” in Telecommunications Energy Conference (INTELEC), 2014 IEEE 36th International, Sept 2014, pp. 1–5.

[2] Protection Against Lightning—Part 4: Electrical and Electronic Systems Within Structures, IEC-62305-4 IEC Standard, Geneva, 2010.

[3] Resistibility of Telecommunication Equipment Installed in Customer Premises to Overvoltages and Overcurrents, ITU-T K.21 ITU-T Recommendation, Geneva, Apr. 2015.,.

[4] Resistibility of Telecommunication Equipment Installed in a Telecommunication Centre to Overvoltages and Overcurrents, ITU-T K.20 ITU-T Recommendation, Geneva, Apr. 2015.

[5] Proteção contra Descargas Atmosféricas - Parte 4: Sistemas Elétricos e Eletrônicos, ABNT NBR 5419, Rio de Janeiro, 2015.

[6] R. Araneo, S. Celozzi, A. Tatematsu, and F. Rachidi, “Time-domain analysis of building shielding against lightning electromagnetic fields,” IEEE Transactions on Electromagnetic Compatibility, vol. 57, no. 3, pp. 397–404, June 2015.

[7] M. Ishii, K. Miyabe, and A. Tatematsu, “Induced voltages and currents on electrical wirings in building directly hit by lightning,” Electric Power Systems Research, vol. 85, pp. 2–6, 2012.

[8] S. Miyazaki and M. Ishii, “Role of steel frames of buildings for mitigation of lightning-induced magnetic fields,” Electromagnetic Com-patibility, IEEE Transactions on, vol. 50, no. 2, pp. 333–339, May 2008.

[9] I. Metwally, F. Heidler, and W. Zischank, “Magnetic fields and loop voltages inside reduced- and full-scale structures produced by direct lightning strikes,” Electromagnetic Compatibility, IEEE Transactions on, vol. 48, no. 2, pp. 414–426, May 2006.

[10] W. J. Zischank, F. Heidler, J. Wiesinger, K. Stimper, A. Kern, and M. Seevers, “Magnetic fields and induced voltages inside lpz 1 measured at a 1:6 scale model building,” in International Conference on Lightning Protection, Avignon, 2004, pp. 1–6.

[11] C. F. Barbosa and J. O. S. Paulino, “A closed expression for the lightning induced voltage in short loops,” IEEE Transactions on Electromagnetic Compatibility, vol. 58, no. 1, pp. 172–179, Feb 2016.

[12] J. O. S. Paulino, P. C. Assuncao, and C. F. Barbosa, “Lightning induced voltages in large loops,” in Lightning Protection (XIII SIPDA), 2015 International Symposium on, Sept 2015, pp. 47–53.

[13] Y. Fuangfung, S. Sinthusonthishat, and P. Yutthagowith, “A soft-ware tool for induced voltages and currents calculation caused by lightning electromagnetic field in pv systems,” in Electrical Engineering/Electronics, Computer, Telecommunications and Information Technology (ECTI-CON), 2015 12th International Conference on, June 2015, pp. 1–4.

[14] I. Metwally and F. Heidler, “Computation of transient overvoltages in low-voltage installations during direct strikes to different lightning protection systems,” Electromagnetic Compatibility, IEEE Transactions on, vol. 49, no. 3, pp. 602–613, Aug 2007.

[15] A. Kern, F. Heidler, M. Seevers, and W. Zischank, “Magnetic fields and induced voltages in case of a direct strike comparison of results obtained from measurements at a scaled building to those of iec 62305-4,” Journal of Electrostatics, vol. 65, no. 56, pp. 379–385, 2007.

[16] V. Hegde and V. Shivanand, “On the influence of steel geometry on the induced currents in steel reinforced concrete building due to a nearby lightning strike to ground,” Electromagnetic Compatibility, IEEE Transactions on, vol. 57, no. 3, pp. 418–424, 2015.

[17] A. Tatematsu, F. Rachidi, and M. Rubinstein, “Analysis of electromagnetic fields inside a reinforced concrete building with layered reinforcing bar due to direct and indirect lightning strikes using the fdtd method,” Electromagnetic Compatibility, IEEE Transactions on, vol. 57, no. 3, pp. 405–417, 2015.

[18] I. Metwally and F. Heidler, “Reduction of lightning-induced magnetic fields and voltages inside struck double-layer grid-like shields,” Electromagnetic Compatibility, IEEE Transactions on, vol. 50, no. 4, pp. 905–912, Nov 2008.